Time-differential perturbed-angular-correlation study of pure and Sn-doped In_2O_3 semiconductors

A. G. Bibiloni, C. P. Massolo, J. Desimoni, L. A. Mendoza-Zélis, F. H. Sánchez, A. F. Pasquevich, L. Damonte, and A. R. López-García

Departamento de Física, Facultad de Ciencias Exactas, Universidad Nacional de La Plata, Calle 49 y 115, 1900 La Plata, Argentina

(Received 19 December 1984)

We present a series of measurements of the static and time-dependent interactions in the angular correlation of ^{111}In (electron capture to ^{111}Cd) in pure and Sn-doped In_2O_3. Results on the static electric field gradient are consistent with mainly ionic bonds and confirm the *s* character of the conduction band. The temperature and free-electron-density dependence of the fluctuating interaction is analyzed, thus allowing a tentative description of electron-capture aftereffects in semiconductors and insulators compounds. The hyperfine parameter characteristic of the time-dependent interaction provides a measurement of the hole lifetime in an impurity level. The position of the Cd impurity level deduced from our results is 0.16_4 eV above the valence band.

I. INTRODUCTION

After the comprehensive work of Haas and Shirley[1] in 1973, the time-differential perturbed-angular-correlation (TDPAC) technique has been increasingly applied to study solid semiconductor compounds. Although all the experiments are based on the measurement of the electric field gradient (EFG) at the probe sites, they have been performed with different aims concerning semiconductor properties. Indeed, while phase transitions were studied in In_2Se_3 (Ref. 2) and V_2O_3 (Ref. 3), Amaral *et al.*[4] investigated the structural changes connected with the electrical switching of InSe, and Unterricker and Schneider[5] were interested in the correlation of the nuclear quadrupole coupling with the tetragonal compression in some chalcopyrite compounds. Also, the radiation damage recovery in semiconductors has been studied[5–7] by TDPAC.

The temperature dependence of the EFG has been studied in several semiconductor compounds in some detail. Different mechanisms have been invoked in an attempt to explain the distinct temperature dependence measured in each compound. In Te,[8] for example, the EFG first remains constant and then increases with temperature. A similar behavior was found in Bi_2Te_3 and Sb_2Te_3.[9] The exponential dependence found in the intrinsic region of these semiconductors led the authors in Ref. 9 to propose a qualitative explanation in which changes in the free-electron density were assumed to be the main mechanism responsible for the variation in the EFG with temperature. Consistent with this description was the nearly constant EFG measured in CdSe, HfO_2 (Ref. 10), and In_2Te_3 (Ref. 9) semiconductors with larger band gaps. On the other hand, Forkel *et al.*[11] found a sharp increase in the EFG in In_2Te_5 around 150 K which they explain in the framework of a bond switching model describing the thermal repopulation of the electronic states in the temperature range of extrinsic conductivity. In a recent paper Amaral *et al.*[12] reported a well-defined change in the temperature dependence of the nuclear quadrupole interaction measured in InSe: From 110 K up to 823 K they found a $T^{3/2}$ dependence, while between 4 and 80 K the EFG varies linearly with temperature. They suggest that this can be related to changes in the dimensionality of the phonon spectrum. It is clearly evident that in nonmetallic systems the temperature dependence of the EFG results from several mechanisms which contribute independently and not a universal law—like the $T^{3/2}$ law in metals—can be extracted.

Another controversial feature of TDPAC measurements in semiconductors is the presence of a time-dependent interaction due to the aftereffects (AE) following the nuclear electron capture (EC) of the probe. This effect is not systematically present in all the semiconductors studied. Indeed, even though all the TDPAC measurements mentioned above—except that on HfO_2 (Ref. 10)—have been performed using ^{111}In probes, which decay by electron capture to ^{111}Cd and hence are subject to electronic relaxation, only one of them ($CdCl_2$ in Refs. 10 and 13) showed an attenuation associated with AE. Aftereffects have also been reported by Haas and Shirley,[1] who studied $Rh(NH_3)_3Cl_3$ [measured with ^{99}Rh(EC)^{99}Ru], Cs_2PdCl_4 [measured with ^{100}Pd(EC)^{100}Rh], and $InPO_4$ (measured with ^{111}In). Also, a recent study of indium chlorides performed by Martin *et al.*[14,15] showed the presence of AE in $InCl_3$, $InCl_2$, and $InCl_{1.8}$. Whether or not the angular correlation measured in a given compound is perturbed by AE is still an open question.

We have presented in a previous work[16] preliminary results of the temperature dependence of electron-capture aftereffects in the semiconductor In_2O_3, suggesting that AE measurements should provide information about local electric properties at impurity sites in semiconductors. Following our investigation, we present in this paper a complete analysis of the temperature dependence of the hyperfine interaction measured in In_2O_3. We also report our results on the In_2O_3:Sn system, with two different Sn

concentrations (0.025 and 1 at. %), measured in the temperature range 14—500 K.

We analyze the complete set of data and discuss not only the temperature dependence of both static and fluctuating interactions, but also their dependence with the free-carrier concentration. Our results show no dependence of the EFG with the free-electron density which confirms the *s* character of the conduction band of the In_2O_3 semiconductor.

Concerning the fluctuating interaction, our results are consistent with the following description of aftereffects: The extremely fast hole diffusion in the valence band leads (in less than 10^{-15} s) the initially highly ionized atom to a state in which only the holes trapped in an impurity level, above the valence band, will remain long enough to modify the angular correlation. The fluctuating interaction which is turned on when the nuclear electron capture occurs, is turned off when the trapped hole recombines with electrons that may come either from the conduction band or from the valence band by thermal excitation. Hence, the relaxation constant λ_g associated with the fluctuating interaction provides a measurement of the lifetime of a hole in a trap center.

II. EXPERIMENTAL PROCEDURE

A. Measurement technique

The TDPAC technique is based on the observation of the influence of extranuclear fields on the correlation between emission directions of two successive radiations emitted during a nuclear decay cascade. Complete description of this and related techniques can be found in the literature.[17] We made use of the radioactive isotope ^{111}In, which decays by electron capture with a 2.8-day half-life to nuclear levels in ^{111}Cd. The major fraction of excited ^{111}Cd produced in this way decays to the ground state by the cascade emission of two γ rays of energies 173 and 247 keV, respectively. The intermediate nuclear level at 247 keV populated by 173-keV transition has nuclear spin $I=\frac{5}{2}$, a half-life of 84 ns, and an electric quadrupole moment of $0.77_{12}b$.[18] Using the conventional formulation,[17] the correlation function is written as

$$W(\theta,t)=1+A_2G_2(t)P_2(\cos\theta)\ , \tag{1}$$

where θ is the angle between the first and second γ-ray emission directions, P_2 is the second-order Legendre polynomial, and higher-order terms can be neglected in the present case. For the cascade in ^{111}Cd, $A_2^{\rm th}=0.18$ is the theoretical angular correlation coefficient, which depends only on the spins of the states and nature of the transitions involved in the nuclear decay. The form of the perturbation factor $G_2(t)$ depends on the nature and time dependence of the fields acting on the nucleus.

B. Sample preparation

1. In_2O_3 compound

A natural cadmium foil was irradiated with 28-MeV deuterons in order to produce the ^{111}In activity through the nuclear reaction ^{110}Cd$(d,n)^{111}$In. After irradiation the cadmium foil was dissolved in HNO_3 together with some indium metal. Then H_2S was bubbled into the solution, and the yellow precipitate of CdS was eliminated by centrifugation. This process was repeated until no visible CdS was present. The solution was then evaporated, and the In_2O_3 was obtained by calcination of $In(NO_3)_3$ at about 770 K. Finally, the compound was annealed in air at 1273 K for six hours. The suitability of the described process was checked through x-ray analysis of the resulting product. The Debye-Scherrer pattern only showed the characteristic lines of In_2O_3 corresponding to the cubic bixbyite structure reported by Swanson *et al.*[19]

2. In_2O_3:Sn compounds

For the In_2O_3:Sn compounds with 0.025- and 1-at. % Sn the method described by Franck *et al.*[20] was employed. That is, Cl_4Sn and Cl_3In solutions with the appropriate molar concentrations were prepared. In the indium chloride solution some commercially obtained Cl_3 ^{111}In activity was included. The solutions were mixed together and uninterruptedly stirred at a constant temperature of 60 °C. The resulting solution was then neutralized to a pH of 7 by addition of NH_4OH. As a consequence of the coprecipitation of indium hydroxide and stannic acid a white homogeneous paste was obtained. The precipitate was filtered and washed several times with NH_4NO_3 to eliminate free Cl^- ions. Finally, calcination treatments in air at 1273 K during 10 h were performed. From activity measurements the concentration of ^{111}In in the final compound was estimated to be less than 10 at. %. The samples were analyzed with an x-ray diffractometer revealing only the bixbyite structure of indium sesquioxide.

C. Data reduction and parametrization

A conventional automatic two detector apparatus was used with one NaI(Tl) and one CsF scintillator, providing a time resolution of 2.4 ns full width at half maximum. After subtraction of chance coincidence background, time spectra corresponding to angles 90° and 180° between detectors were combined to form the ratio

$$R(t)=2\frac{N(180°,t)-N(90°,t)}{N(180°,t)+2N(90°,t)}=A_2^{\rm expt}G_2(t)\ . \tag{2}$$

Theoretical functions of the form $A_2G_2(t)$, folded with the measured time resolution curve, were fitted to the experimental asymmetry ratios $R(t)$. The perturbation factor $G_2(t)$ takes into account two different hyperfine interactions: the static one due to the coupling of the nuclear quadrupole moment and the electric field gradient of the charge distribution in the lattice, and the time-dependent interaction associated with AE.

Since there are two nonequivalent sites for the In atoms in the In_2O_3 lattice, the perturbation factor corresponding to the static interaction will be of the form

$$G_2^s(t)=\sum_{i=1}^{2}f_i\sum_{n=0}^{3}s_{n,i}\exp(-\delta_i\omega_{n_i}t)\cos(\omega_{n_i}t)\ , \tag{3}$$

where f_i are the relative fractions of nuclei that experi-

ence a given perturbation. The frequencies ω_n are related by $\omega_n = F_n(\eta)\omega_Q$ to the quadrupole frequency $\omega_Q = eQV_{zz}2\pi/40h$. The coefficients F_n and s_n are known functions[21] of the axial symmetry parameter η defined by $\eta = (V_{xx} - V_{yy})/V_{zz}$, where V_{ii} are the principal components of the EFG tensor. The exponential function accounts for a Lorentzian frequency distribution of relative width δ around ω_n.

Concerning the time-dependent interaction, use has been made of the perturbation factor derived by Bäverstam *et al.*[22] on the basis of the Abragam and Pound[23] theory. The authors in Ref. 22 have shown that the basic assumptions of the Abragam and Pound theory are satisfied in AE processes and derived a modified perturbation factor by taking into account the fact that the fluctuating interaction is turned off when the atomic ground state is reached. To do so, two simplifying assumptions were made.

(i) The probability for an atom to reach its ground state in the time interval t, $t+dt$ is given by

$$P_g(t)dt = \lambda_g \exp(-\lambda_g t)dt \ . \tag{4}$$

This assumption implies that the whole atomic recovery process is characterized by a single exponential recovery time λ_g^{-1}.

(ii) The mean interaction strength, characterized by the Abragam and Pound relaxation constant λ_r, remains constant during the time the holes are bound to the probe.

The time-dependent contribution to the perturbation factor can be written then as

$$G_2^*(t) = \frac{\lambda_g}{\lambda_g+\lambda_r} + \frac{\lambda_r}{\lambda_g+\lambda_r}\exp[-(\lambda_g+\lambda_r)t] \ . \tag{5}$$

When the complete atomic recovery is achieved, the hyperfine interaction becomes static. Since this interaction is much weaker than the time-dependent one, $G_2(t)$ can be expressed as the product[22]

$$G_2(t) = G_2^s(t)G_2^*(t) \ . \tag{6}$$

III. RESULTS AND DISCUSSION

A. Static electric field gradient

As we reported in Ref. 24, two static quadrupole interactions, with relative amplitude ratio 3:1, are present in In_2O_3, corresponding to the two inequivalent indium sites in the oxide structure. In Fig. 1 the quadrupole frequencies ω_Q for each indium site of pure In_2O_3 are plotted versus temperature. No dependence of the quadrupole parameters with temperature is observed. The frequencies distributions, not shown in the figure, were 1% or less for both interactions throughout the studied temperature range. Despite a slight dispersion in the fitted values of the asymmetry parameter η_2, it was also found temperature independent. A fixed value of $\eta_2 = 0.12$ was adopted in the fits shown in Fig. 1.

The measured quadrupole parameters at RT are reported in Table I together with the corresponding principal component V_{zz} of the electric field gradient (EFG) deduced by assuming a Sternheimer factor $(1-\gamma_\infty) = 30.3$.[25] The experimental electric field gradients are also compared with those predicted from a ionic point-charge model. We have also made calculations based on a covalent approach, which are discussed elsewhere,[26] but an ionic model seems to be more realistic since the structure adopted by In_2O_3—a defect fluorite one—is rather indicative of mainly ionic bonds. The point-charge calculation was performed summing over the first 30 nearest neighbors using the atomic coordinates and cell parameters reported by Marezio[27] and charges -2 and $+3$ at O and In sites, respectively. A summation over the whole lattice using the De Wette method yields similar results. Despite the simplifications involved in the model, the agreement with measured values of V_{zz} and η is fairly good. In particular, it correctly predicts the observed ratio between the principal values of EFG at both In sites. We infer then, that the observed EFG is mainly originated at the ionic lattice. This is strongly supported by the constancy of the quadrupole parameters with temperature (see Fig. 1) which shows none of the typical behaviors of electronic contributions to EFG. According to Ref. 28 the electron concentration should increase at low temperatures due to the ionization of the oxygen vacancies donor levels ($\epsilon \sim 0.03$ eV) and a further increase should be noticeable above 1000 K where the dissociation reaction provides more oxygen vacancies (see also Ref. 29). The absence of any change in the ω_Q values for In_2O_3 would then indicate the s character of these free electrons.

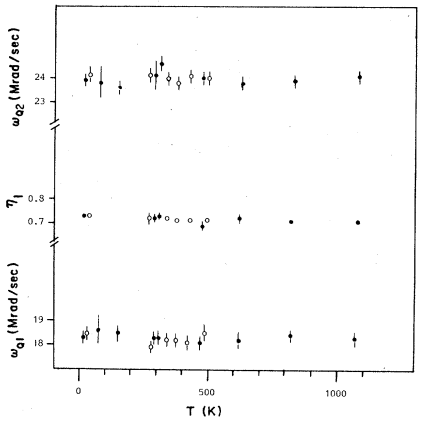

FIG. 1. Temperature dependence of the fitted quadrupole parameters in pure (●) and 0.025-at. % Sn-doped (○) In_2O_3 compounds.

In this respect it is worthwhile to discuss now the results obtained on Sn-doped In_2O_3, also reported in Table I, where an estimation of the corresponding free-carrier densities n is quoted. The free-electron concentration value for pure In_2O_3 is the average of those reported by Weiher,[28] measured in four different samples. For the tin-doped compounds we estimated the free-carrier concentration, basing our calculation on the results of Köstlin *et al.*[30] They showed that for low Sn concentration every tin atom is substitutionally incorporated at an In^{3+} site as an Sn^{4+} ion giving one free electron (since all these impurities are ionized at RT). As can be seen in Table I the quadrupole parameters do not vary significantly with the

TABLE I. Fitted quadrupole parameters to RT measurements of pure and Sn-doped In_2O_3 samples. The calculated parameters for In_2O_3 are also shown for comparison. The free-electron-density (n) values are estimated as explained in the text.

Sample	n (cm^{-3})	ω_{Q1} (10^6 rad/sec)	$V_{zz}^{(1)}$ (10^{16} V/cm^2)	η_1	δ_1 (%)	ω_{Q2} (10^6 rad/sec)	$V_{zz}^{(2)}$ (10^{16} V/cm^2)	η_2	δ_2 (%)	$\frac{V_{zz}^{(2)}}{V_{zz}^{(1)}}$
$In_2O_3^{calc}$			1.7	0.54			2.2	0.0		1.36
In_2O_3	6.0×10^{17}	18.3_3	2.1_3	0.72_2	0_1	24.3_6	2.7_4	0.12	0_1	1.33
In_2O_3:Sn 0.025 at. %	8.2×10^{18}	17.9_3	2.0_3	0.72_2	1_1	24.1_3	2.7_4	0.12	0_2	1.35
In_2O_3:Sn 1 at. %	3.0×10^{20}	18.3_2	2.1_3	0.73_1	4_1	23.9_2	2.7_4	0.18_2	1_1	1.31

number of electrons in the conduction band. The slight variation in η_2 can be understood in the framework of an ionic model.[26]

These results provide evidence for the *s* character of the conduction band, since otherwise the conduction electrons would give a significant contribution to the EFG. In addition the observed quadrupole parameters are temperature independent (from 14 to 473 K and 14 K to RT for samples with 0.025- and 1-at. % Sn, respectively), see Fig. 1, supporting our conclusions and confirming the schematic energy band diagram given by Fan and Goodenough[31] (see Fig. 5).

B. Time-dependent interaction

We have reported in a recent paper[16] a TDPAC measurement of electron-capture aftereffects in the semiconductor In_2O_3. Aftereffects are characterized by a time-dependent interaction which is turned off when the atomic recovery is achieved. The temperature dependence of AE, which reveal a faster atomic recovery with increasing temperature, was interpreted in terms of the electron availability increment at the probe's site. In order to test this interpretation, we continue our investigation measuring the time-dependent interaction as a function of the electron density in the conduction band doping In_2O_3 with Sn impurities. As we mentioned in Sec. III A, at low Sn concentration, every impurity atom incorporates one quasifree electron in a single donor level at less than 0.03 eV below the conduction-band edge. In Fig. 2 we show TDPAC spectra corresponding to three different Sn concentrations, measured at RT where all the impurities are ionized. The spectrum (a), obtained with an undoped In_2O_3 sample, is clearly dominated by the exponential at-

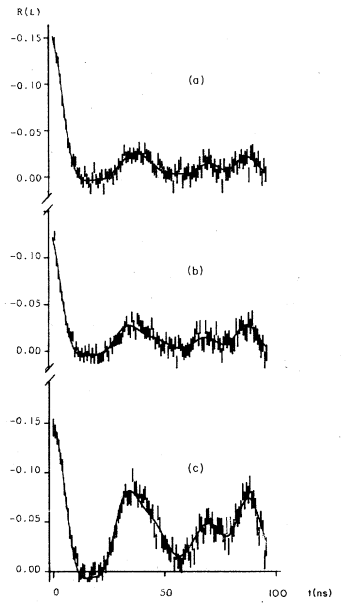

FIG. 2. TDPAC spectra, measured at RT, of (a) undoped In_2O_3, (b) 0.025-at. % Sn-doped In_2O_3, and (c) 1-at. % Sn-doped In_2O_3. The solid curves are least-squares fits of Eq. (6) to the data.

tenuation characteristic of the time-dependent interaction. In sample (b) the free-carrier density has been increased by a factor 10 by the addition of 0.025 at. % of Sn impurities. A time-dependent interaction can still be recognized although the exponential attenuation of the angular correlation is much weaker. The last spectrum (c), corresponds to a 1-at. % Sn doping which means an increase of 10^3 times in the free-electron-density respect to the pure compound. Here, no time-dependent interaction is present. Only the two well-defined static quadrupole interactions of the In_2O_3 compound can be recognized. When this sample is measured at 14 K, where not all the impurities are ionized, the time-dependent interaction is observed.

The hyperfine parameters that characterize the fluctuating interaction, λ_g and λ_r, have been defined in Sec. II C. In Fig. 3 we show the temperature dependence of these parameters measured in In_2O_3: pure (●), doped with 0.025-at. % (○), and 1-at. % (■) Sn impurities.

The Abragam and Pound relaxation constant λ_r was found temperature independent in both compounds throughout the temperature range studied. The measured λ_r are slightly dispersed around a mean value of $\lambda_r = 0.12$ ns^{-1}. The parameter λ_r takes into account all the fluctuating interactions which are present during the atomic recovery, for example, the spin-lattice relaxation and the electronic disturbances in the probe's surrounding. Since the correlation times arising from these mechanisms are all contained in the single quantity λ_r, it is very difficult to obtain any quantitative information about the processes involved from the measured λ_r values shown in Fig. 3. Nevertheless, it can be worth mentioning that the λ_r measured value (0.12 ns^{-1}) is consistent with a calculated estimation of the magnitude of the Abragam and Pound constant associated with a pure magnetic interaction produced by a hole in the $4d$ shell of the Cd atom. Assuming a typical value of the correlation time of 2×10^{-12} s, and a magnetic field at the nucleus of 0.3 MG (average value of the magnetic field calculated for the $4d$ shell in a hydrogenic model with screened effective nuclear charge), one obtains $\lambda_r = 0.2$ ns^{-1}, which is, as we stated, consistent with the measured values.

The parameter λ_g is the probability, per unit time, for an atom to reach its ground state (the normal ionization state Cd^{2+}). As can be seen in Fig. 3, the λ_g values measured in the Sn-doped samples are systematically higher than those measured in pure In_2O_3. A quite similar temperature dependence of λ_g is found in both compounds. In Fig. 4 we show the fraction of atoms $N_i = \exp(-10\lambda_g)$ that still have a nonequilibrium ionization after the first 10 ns ($t = 0$ is given by the detection of the first γ of the cascade), calculated using the λ_g values of Fig. 3. In both compounds the temperature dependence of the atomic recovery is clearly similar. The fraction of ionized probes is lower in the doped compound than in the pure In_2O_3 throughout the temperature range studied. In particular, at 500 K, while in the Sn-doped sample all the ions have reached its ground state, there are more than 50% still ionized probes in the undoped indium sesquioxide.

It is clear from the results shown in Figs. 3 and 4 that the parameter which reveals both the temperature and free-electron-density dependence of AE is λ_g, that is the atomic recovery constant. Let us then consider how the atomic recovery constant depends on (i) the final number of holes after the electronic relaxation following the nuclear electron capture, (ii) the position of the hole levels in the band structure of the semiconductor, and (iii) the electron supply.

Concerning the number of holes, a brief description of the processes involved after a nuclear electron capture can be of use. After formation of the K hole, atomic shell and nucleus tend to reach their ground state: the nucleus by decaying through the γ-γ cascade, the atomic shell by releasing the excitation energy through emission of Auger electrons and x rays. A hole in the K shell moves very rapidly to the outermost shell. This movement occurs mainly through Auger transitions and hence more holes are created that also move outward. The total time required for a hole to move out to the outermost shell is of the order of 10^{-14}–10^{-15} s. Since the half-life of the initial state of the γ cascade is 1.2×10^{-10} s, the relaxation of the inner holes to the outermost shells takes place before the emission of the first γ ray. Experimental investigations show that the average charge of an atom after K capture is quite large. One expects for Cd an average charge of approximately $7e^-$, although individual Cd atoms may acquire much higher charges.[17] The number of holes is determined by atomic processes and should not

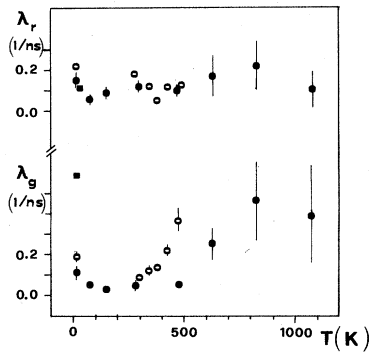

FIG. 3. Temperature dependence of the hyperfine parameters characteristic of the time-dependent interaction in undoped (●), 0.025-at. % Sn-doped (○), and 1-at. % Sn-doped (■) In_2O_3 samples.

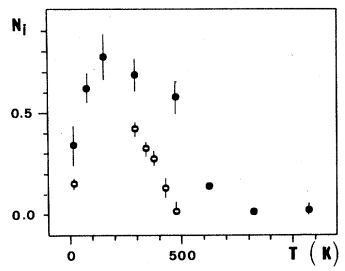

FIG. 4. Temperature dependence of the number of atoms still ionized 10 ns after the emission of the first γ ray of the cascade, derived from the values shown in Fig. 3. ●, In_2O_3; ○, In_2O_3:Sn (0.025 at. %).

vary either with temperature or with the addition of Sn impurities.

In order to discuss the position of the hole levels we will give in the following a brief description of the In_2O_3 band structure. As prepared, indium oxide is generally somewhat reduced. At each oxygen vacancy (V_o) symmetrized In:5*s* orbitals form shallow donor states just below E_c that trap two electrons per oxygen vacancy. When tin is incorporated in a substitutional In site of In_2O_3, the larger nuclear charge of the impurity atom stabilizes a single donor level just below E_c. In Sn-doped In_2O_3, V_o and Sn^{3+} donor levels should coexist and both provide electrons to the conduction band. The schematic energy-band model proposed by Fan and Goodenough[31] is shown in Fig. 5.

In our case, where ^{111}In radiative probes are incorporated in the semiconductor, the nuclear decay creates in the In_2O_3 lattice a Cd^{3+} impurity which introduces a single acceptor level in the band gap. To our knowledge, the position of this Cd acceptor level in In_2O_3 has neither been measured nor calculated.

In a very naive model, supposing that the sudden creation of a number of holes will not modify the band structure of the semiconductor, one can expect that all the holes should lie inside the valence band, except one which would be in the single acceptor level mentioned above. If so, all but one of these holes can diffuse in the valence band.

In order to evaluate the diffusion time we have studied the unidimensional diffusion equation with a delta function with support at the origin as initial hole concentration; this corresponds to a situation where all holes are located at the Cd atom. We want to determine $t_{1/2}$, the time after which half of the holes still remain in a region of width $2r$ centered at the origin. Calling $C(x,t)$ the concentration at the point x at time t, and from the relation

$$\frac{C_0}{2}=\int_{-r}^{r} C(x,t_{1/2})dx \ , \tag{7}$$

where C_0 is the initial concentration and using the solution of the diffusion equation, we obtain from Eq. (7)

$$\frac{1}{2}=\phi\left[\frac{r}{2(t_{1/2}D)^{1/2}}\right] , \tag{8}$$

where ϕ is the error function[32] and D, the diffusion coefficient,[33] is given by the Einstein relationship

$$D=k_B T\mu_h/q \ , \tag{9}$$

where μ_h is the hole mobility, k_B is the Boltzmann constant, and q is the electron's charge. To our knowledge, the hole mobility in In_2O_3 has not been measured, and therefore it is not possible to compute $t_{1/2}$ in our case. Assuming a hole mobility as low as 1 cm^2/Vs, one obtains a $t_{1/2}$ value of the order of 10^{-14} s. This is several orders of magnitude shorter than the lifetime of the first nuclear state of the γ cascade. Hence, no perturbation of the angular correlation should arise from holes initially located inside the valence band. If this is true, no aftereffects should be present in cadmium compounds measured with ^{111}In probes (nor in those compounds where Cd is an isovalent impurity). This is verified in all the cadmium compounds reported in the literature with the exception of $CdCl_2$.[10] The authors in Ref. 10 claim that AE are responsible for the strong attenuation of the angular correlation in $CdCl_2$ when measured with ^{111}In probes. It would be very interesting to perform TDPAC measurements of this insulator as a function of temperature, which would give conclusive results concerning the origin of the observed attenuation.

All the above considerations lead us to infer that only the holes trapped in levels above the valence band can originate time-dependent perturbations to the nuclear angular correlation.

A careful analysis of the semiconductors and insulators measured by TDPAC where the radiative probes decaying by electron capture introduce an acceptor level, suggests a correlation of aftereffects with the spatial distribution of valence electrons. Actually, aftereffects have never been reported in tetrahedrally coordinated ("covalent") semiconductors. Instead, in all the compounds showing AE the probes have a coordination higher than four with mainly ionic bonds.

To summarize the above discussion we can say that the relevant parameters in aftereffects measurements are not the number of holes introduced due to the nuclear electron capture but the position of the hole levels in the band configuration of the compound. Only holes trapped in impurity levels must be considered. Moreover, aftereffect at-

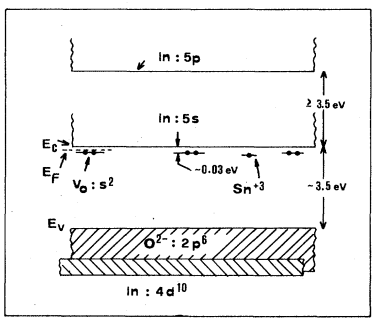

FIG. 5. Schematic energy-band model for Sn-doped In_2O_3, having no Sn_3O_4-like phase, for small Sn concentrations, given by Fan and Goodenough (Ref. 31).

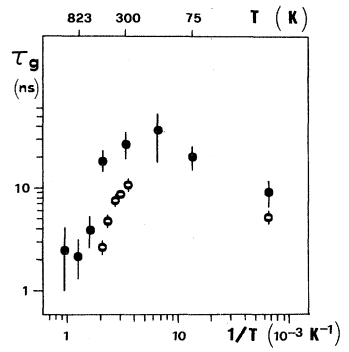

FIG. 6. Temperature dependence of the hole lifetime in the impurity level for undoped (●) and 0.025-at. % Sn-doped (○) In_2O_3, in a semilogarithmic plot.

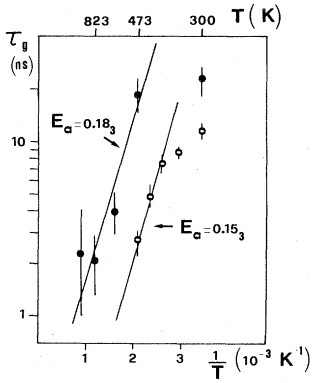

FIG. 7. Same as Fig. 6 in expanded scale to show the high-temperature region.

tenuation of the angular correlation seems to be related to the spatial distribution of the valence electrons.

Finally, let us discuss the dependence of λ_g on the electron supply to the impurity level. In our case, at low temperatures electrons are provided basically by the conduction band. At increasing temperatures the thermal excitation of electrons from the valence band to the impurity level becomes predominant. Since the fluctuating interaction is turned off when the atomic recovery is achieved, the hyperfine parameter $\tau_g = 1/\lambda_g$ provides the lifetime of the hole trapped in the impurity level. We show in Fig. 6 the measured lifetime in In_2O_3 pure (●) and 0.025-at. % Sn doped (○), versus $1000/T$. A well-defined change in the temperature dependence was found. The hole recombination with electrons coming from the conduction band, is the main mechanism at low temperature. The increment of τ_g with temperature which is observed between 14 and 150 K, may be related to electron-phonon interaction effects. The fact that the measured lifetime in the Sn-doped compound is systematically shorter than the corresponding one in pure In_2O_3 reveals that the low-temperature mechanism is also present at high temperatures. Around 150 K the thermal excitation of electrons from the valence band becomes important. The high-temperature region in Fig. 6 is expanded in Fig. 7. The linear behavior in the chosen scales suggests an exponential temperature dependence of the hole lifetime. Within errors and taking into account only the high-temperature points the same slope can be fitted for both In_2O_3 and In_2O_3:Sn experimental set of τ_g values. A mean value of 0.16_4 eV can therefore be assigned to the cadmium impurity acceptor level.

IV. CONCLUSIONS

We have studied by TDPAC the static and time-dependent hyperfine interaction in pure and Sn-doped In_2O_3. The magnitude and temperature dependence of the static electric field gradients reveal the ionic character of the bonds. No dependence of the EFG was found with the free-electron density, confirming the *s* character of the conduction band. Our results are in agreement with the schematic energy-band diagram given by Fan and Goodenough.[31]

Concerning the time-dependent interaction the objective of this paper was to give some insight to aftereffects processes in semiconductors and insulators. The analysis of our results and those reported in the literature suggest the following tentative conclusions. Only the holes trapped in levels above the valence band perturb the angular correlation. Hence, only in those cases in which the nuclear electron capture introduces an impurity acceptor level in the band structure of the compound, might the time-dependent interaction be observed. A further requirement (based only on the scarce available experimental data) seems to be a predominantly ionic character of the bonds. In this framework, the relevant parameter τ_g which characterizes the fluctuating interaction provides a measurement of the lifetime of a hole trapped in the impurity level. Results obtained in the high-temperature region, give a tentative value of 0.16_4 eV for the position of the cadmium impurity level above the valence band. Further investigations are in progress in order to confirm the picture described above.

ACKNOWLEDGMENTS

The authors wish to thank Professor H. Fanchiotti for fruitful discussions and comments. The assistance of Licenciado Luis Terminiello in the sample preparation is greatly appreciated. This work was partially supported by Consejo Nacional de Investigaciones Científicas y Técnicas (CONICET), Comisión de Investigaciones Científicas de la Provincia de Buenos Aires (CICPBA), Subsecretaría de Ciencia y Técnica (SUBCYT), Argentina, and Kernforschungszentrum Karlsruhe Gesellschaft mit bestchränkter Haftung, West Germany.

[1]H. Haas and D. A. Shirley, J. Chem. Phys. **58**, 3339 (1973).
[2]K. Krusch and J. Gardner, Phys. Rev. B **24**, 4587 (1981).
[3]M. Forker, H. Saitovitch, and P. R. De Jesus Silva, Hyperfine Interac. **15/16**, 809 (1983).
[4]L. Amaral, M. Behar, A. Maciel, L. S. de Oliveira, and W. H. Schreiner, J. Phys. C **16**, L1039 (1983).
[5]S. Unterricker and F. Schneider, Hyperfine Interac. **15/16**, 827 (1983).
[6]S. Unterricker and F. Schneider, Phys. Status Solidi A **75**, 155 (1983).
[7]S. Unterricker, P. Hlídek, M. Zvára, and F. Schneider, Phys. Status Solidi B **102**, K27 (1980).
[8]H. Barfuss, G. Böhnlein, H. Hohenstein, W. Kreische, H. Niedrig, and A. Reiner, Z. Phys. B **45**, 193 (1982).
[9]H. Barfuss, G. Böhnlein, F. Gubitz, W. Kreische, and B. Röseler, Hyperfine Interac. **15/16**, 815 (1983).
[10]H. Barfuss, G. Böhnlein, H. Hohenstein, W. Kreische, H. Niedrig, H. Appel, R. Heidinger, J. Randies, G. Then, and W.-G. Thies, Z. Phys. B **47**, 99 (1982).
[11]D. Forkel, W. Engel, H. Iwatschenko-Borho, R. Keitel, and W. Witthuhn, Hyperfine Interac. **15/16**, 821 (1983).
[12]L. Amaral, M. Behar, A. Maciel, and H. Saitovitch, Phys. Lett. **102A**, 45 (1984).
[13]H. Barfuss, G. Böhnlein, H. Hohenstein, W. Kreische, H. Niedrig, H. Appel, J. Randies, and W. G. Thies, Hyperfine Interac. **10**, 963 (1981).

[14]P. W. Martin, S. R. Dong, and J. G. Hooley, Hyperfine Interac. **15/16**, 933 (1983).
[15]P. W. Martin, S. R. Dong, and J. G. Hooley, Chem. Phys. Lett. **105**, 343 (1984).
[16]A. G. Bibiloni, J. Desimoni, C. P. Massolo, L. A. Mendoza-Zélis, A. F. Pasquevich, F. H. Sánchez, and A. R. López-García, Phys. Rev. B **29**, 1109 (1984).
[17]See, for example, H. Frauenfelder and R. M. Steffen, in *Alpha-, Beta-, and Gamma-Ray Spectroscopy,* edited by K. Siegbahn (North-Holland, Amsterdam 1966), pp. 997 and 1182.
[18]R. S. Raghavan, P. Raghavan, and J. M. Friedt, Phys. Rev. Lett. **30**, 10 (1973).
[19]H. E. Swanson, N. T. Gilfrich, and G. M. Ugrimic, Nat. Bur. Stand. (U.S.) Circ. No. 539 (U.S. GOP, Washington, D.C., 1955), Vol. 5, p. 27.
[20]G. Franck, R. Olazcuaga, and A. Rabenau, Inorg. Chem. **16**, 1251 (1977).
[21]L. A. Mendoza-Zélis, A. G. Bibiloni, M. C. Caracoche, A. López-García, J. A. Martínez, R. C. Mercader, and A. F. Pasquevich, Hyperfine Interac. **3**, 315 (1977).
[22]U. Bäverstam, R. Othaz, N. de Sousa, and B. Ringström, Nucl. Phys. **A186**, 500 (1972).
[23]A. Abragam and R. V. Pound, Phys. Rev. **92**, 943 (1953).
[24]J. Desimoni, A. G. Bibiloni, L. Mendoza-Zélis, A. F. Pasquevich, F. H. Sánchez, and A. López-García, Phys. Rev. B **28**, 5739 (1983).
[25]F. D. Feiock and W. R. Johnson, Phys. Rev. **187**, 39 (1969).
[26]R. C. Mercader, F. H. Sánchez, L. A. Mendoza-Zélis, L. Terminiello, A. G. Bibiloni, C. P. Massolo, J. Desimoni, and A. R. López-García, Hyperfine Interac. (to be published).
[27]M. Marezio, Acta Crystallogr. **20**, 723 (1966).
[28]R. L. Weiher, J. Appl. Phys. **33**, 2834 (1962).
[29]J. H. W. De Wit, G. Van Unen, and M. Lahey, J. Phys. Chem. Solids **38**, 819 (1977).
[30]H. Köstlin, R. Jost, and W. Lems, Phys. Status Solidi A **29**, 87 (1975).
[31]J. C. C. Fan and J. B. Goodenough, J. Appl. Phys. **48**, 3524 (1977).
[32]M. Abramowitz and I. Stegun, *Handbook of Mathematical Functions* (Dosen, New York, 1972).
[33]J. L. Moll, in *Physics of Semiconductors,* edited by H. Heffner and A. E. Siegman (McGraw-Hill, New York, 1964), p. 67.